ELSEVIER

Available online at www.sciencedirect.com

SCIENCE DIRECT®

International Journal of Solids and Structures 43 (2006) 3484–3497

INTERNATIONAL JOURNAL OF SOLIDS and STRUCTURES

www.elsevier.com/locate/ijsolstr

Compression stiffness of circular bearings of laminated elastic material interleaving with flexible reinforcements

Hsiang-Chuan Tsai *

Department of Construction Engineering, National Taiwan University of Science and Technology, P.O. Box 90-130, Taipei 106, Taiwan

Received 27 February 2005; received in revised form 18 May 2005
Available online 14 July 2005

Abstract

The compression stiffness of a circular bearing that consists of laminated elastic layers interleaving with flexible reinforcements is derived in closed form. The effect of bulk compressibility in the elastic layer and the effect of boundary condition at the ends of the bearing are considered. The stiffness of the bearing with monotonic deformation is derived first. Then, the bearings with both ends being free from shear force and the bearings with both ends being bonded to rigid plates are studied. The theoretical solutions to the compression stiffness of the bearings are extremely close to the results obtained by the finite element method, which proves that the displacement assumptions utilized in the theoretical derivation are reasonable.

Keywords: Bonded elastic layer; Elastomeric bearing; Seismic isolation

1. Introduction

The laminated rubber bearing typically used for seismic isolation is composed of many layers of elastomer reinforced by steel plates. The reinforcing plates constrain the elastomer from lateral expansion and provide high compression and bending stiffness, but have no effect on the shear stiffness. To analyze the stiffness of the steel-reinforced bearing, the steel reinforcement is treated as completely rigid. Gent and Lindley (1959) derived the compression stiffness of an incompressible elastic layer bonded to rigid plates for infinite-strip shape and circular shape. Subsequently, Gent and Meinecke (1970) extended this method

* Tel.: +886 2 27376581; fax: +886 2 27376606.
E-mail address: hctsai@mail.ntust.edu.tw

0020-7683/$ - see front matter
doi:10.1016/j.ijsolstr.2005.05.012

to analyze the compression stiffness and tilting stiffness of incompressible elastic layers for square and other shapes.

Although rubber can be treated as incompressible in some analyses, the assumption of incompressibility tends to overestimate the stiffness of the bonded rubber layer when the layer's shape factor (defined as the ratio of the one bonded area to the force-free area) is high. Kelly (1997) developed a 'pressure solution' approach to derive the compression stiffness and the tilting stiffness considering the effect of bulk compressibility. The solutions are available for the layers of infinite-strip shape (Chaihoub and Kelly, 1991), circular shape (Chaihoub and Kelly, 1990) and square shape (Koh and Kelly, 1987).

Lindley (1979a,b) applied an energy method to derive the compression stiffness and tilting stiffness of the infinite-strip and circular shapes for the material of any Poisson's ratio. Koh and Kelly (1989) utilized a 'variable transform' approach to derive the compression stiffness of the square shape for compressible material, which is then applied to solve the compression stiffness of the rectangular shape by Koh and Lim (2001). Tsai and Lee (1998, 1999) developed a pressure approach to derive the compression stiffness and tilting stiffness of bonded elastic layers in infinite-strip, circular and square shapes. Recently, that approach was extended to solve the tilting stiffness of circular shape (Tsai, 2003) and the compression stiffness of rectangular shape (Tsai, 2005). These solutions are accurate for materials of any Poisson's ratio.

Steel-reinforced bearings are heavy and expensive. Thus Kelly (1999) suggests that eliminating the steel reinforcing plates and replacing them with fiber reinforcement can significantly reduce both the weight and the cost of isolation bearings. In contrast to the steel reinforcement that is assumed to be rigid, the fiber reinforcement is flexible in extension. Tsai and Kelly (2001, 2002a,b) derived the compression stiffness and tilting stiffness of fiber-reinforced bearings of infinite-strip, circular and rectangular shapes by assuming that the elastomeric layer is incompressible and the reinforcement is flexible. Recently, bulk compressibility is included in the stiffness analysis of fiber-reinforced isolators of infinite-strip shape (Kelly, 2002; Kelly and Takhirov, 2002). In these studies, the flexible reinforcements in the bearing are assumed to have the same deformation, which implies that every elastic layer in the bearing has the same compression stiffness, referred to as 'monotonic deformation' here.

Unlike bearings with rigid reinforcements, where each bonded elastic layer has the same compression stiffness, deformation of flexible reinforcements will cause the compression stiffness of each bonded elastic layers to be different. The boundary condition at the ends of the fiber-reinforced bearings can also affect the compression stiffness. When performing the compression analysis of the bearing subjected to vertical loading only, two types of boundary conditions can be imposed at the ends of the bearing. The first type is that the end of the bearing does not have any horizontal constraint so that it is free from any shear force, referred to here as 'free end'. The second type is that the end of the bearing is bonded to rigid plate so that it does not have any horizontal deformation, referred to here as 'rigid end'.

Recently, a theoretical approach that considers the effect of bulk compressibility in the elastic layer and the effect of boundary condition at the ends of the bearing was developed by Tsai (2004) to derive the compression stiffness of fiber-reinforced bearings in infinite-strip shape. In this current paper, the same method is applied to derive the compression stiffness of fiber-reinforced bearings in circular shape. The stiffness of the circular bearing with monotonic deformation is derived first. Then, the free-end bearings and the rigid-end bearings are studied. In addition to the theoretical derivation, finite element analyses on the fiber-reinforced circular bearings are carried out to verify the exactness of the theoretical solution.

2. Governing equations

The circular bearing shown in Fig. 1 consists of n elastic layers interleaved with flexible reinforcing sheets with elastic layer 1 at the top of the bearing and elastic layer n at the bottom. The reinforcements are counted from 0 to n. The radius of the bearing is b and each elastic layer has the same thickness t. Under

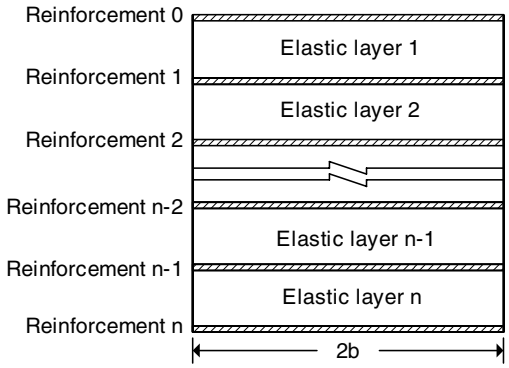

Fig. 1. Bearing consisting of n elastic layers interleaving with reinforcements.

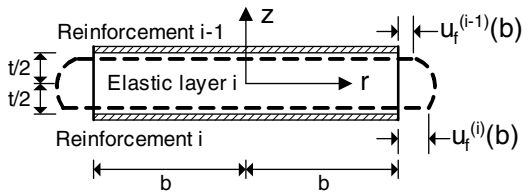

Fig. 2. Deformation of elastic layer.

the axial load in the vertical direction, the bearing is in the axisymmetric stress state. Fig. 2 shows that the deformation of the elastic layer i bonded between the reinforcements $i-1$ and i. A cylindrical coordinate system (r,θ,z) is located at the center of the layer. Under the assumption that the vertical lines in the elastic layers become quadratic-varied after loading, the horizontal displacement of the elastic layer i in the r direction, $u^{(i)}$, can be expressed as

$$u^{(i)}(r,z)=\bar{u}^{(i)}(r)\left(1-\frac{4z^2}{t^2}\right)+u_f^{(i-1)}(r)\left(\frac{1}{2}+\frac{z}{t}\right)+u_f^{(i)}(r)\left(\frac{1}{2}-\frac{z}{t}\right) \tag{1}$$

where $u_f^{(i-1)}(r)$ and $u_f^{(i)}(r)$ are the reinforcement displacements at the top and bottom of the elastic layer i, and the term of $\bar{u}$ represents the bulge deformation. Under the assumption that horizontal planes in the elastic layers remain horizontal, the vertical displacement of the elastic layer i, $w^{(i)}$, is a function of z only

$$w^{(i)}(r,z)=\bar{w}^{(i)}(z) \tag{2}$$

For the isotropic elastic layer i, the pressure $p^{(i)}$ has the following relation with the displacements

$$p^{(i)}(r,z)=-\kappa\left(u^{(i)}_{,r}+\frac{u^{(i)}}{r}+w^{(i)}_{,z}\right) \tag{3}$$

where κ is the bulk modulus and the commas imply differentiation with respect to the indicated coordinate. Define the effective pressure $\bar{p}^{(i)}$ as

$$\bar{p}^{(i)}(r)=-\frac{1}{t}\int_{-t/2}^{t/2}p^{(i)}(r,z)\,\mathrm{d}z \tag{4}$$

Substituting Eqs. (1) and (2) into Eq. (3), the effective pressure becomes

$$\frac{\bar{p}^{(i)}}{\kappa} = -\left[\frac{2}{3}\left(\bar{u}^{(i)}_{,r} + \frac{\bar{u}^{(i)}}{r}\right) + \frac{1}{2}\left(u^{(i-1)}_{f,r} + \frac{u^{(i-1)}_f}{r}\right) + \frac{1}{2}\left(u^{(i)}_{f,r} + \frac{u^{(i)}_f}{r}\right) - \varepsilon^{(i)}_c\right] \tag{5}$$

where $\varepsilon^{(i)}_c$ is the effective compression strain of the elastic layer i defined as

$$\varepsilon^{(i)}_c = -\frac{1}{t}\left[\bar{w}^{(i)}(t/2) - \bar{w}^{(i)}(-t/2)\right] \tag{6}$$

The equilibrium equation in the r direction has the form (Tsai and Lee, 1998)

$$\frac{p^{(i)}_{,r}}{\kappa} = \frac{\mu}{\lambda + 2\mu}(u^{(i)}_{,zz} - w^{(i)}_{,rz}) \tag{7}$$

where λ and μ are Lame's constants. Then, substituting Eqs. (1) and (2) into Eq. (7) and integrating the result through the thickness of the layer leads to

$$\frac{\bar{p}^{(i)}_{,r}}{\kappa} = -\frac{2}{3}\alpha_0^2\bar{u}^{(i)} \tag{8}$$

with

$$\alpha_0 = \frac{1}{t}\sqrt{\frac{12\mu}{\lambda + 2\mu}} \tag{9}$$

The thickness of the reinforcements t_f is much smaller than the thickness of the elastic layers, so that the stresses in the reinforcements can be regarded as a plane stress state in the r–θ plane. Let $N^{(i)}_{rr}$ and $N^{(i)}_{\theta\theta}$ represent the normal forces of the reinforcement i in the r and θ directions, respectively. The force–displacement relations in plane stress state give

$$N^{(i)}_{rr} = \frac{E_f t_f}{1 - v_f^2}\left(u^{(i)}_{f,r} + v_f\frac{u^{(i)}_f}{r}\right) \tag{10}$$

$$N^{(i)}_{\theta\theta} = \frac{E_f t_f}{1 - v_f^2}\left(\frac{u^{(i)}_f}{r} + v_f u^{(i)}_{f,r}\right) \tag{11}$$

where E_f and v_f are the elastic modulus and Poisson's ratio of the reinforcement, respectively. The equilibrium equation of the reinforcement i in the r direction is

$$\frac{\mathrm{d}N^{(i)}_{rr}}{\mathrm{d}r} + \frac{1}{r}(N^{(i)}_{rr} - N^{(i)}_{\theta\theta}) + \tau^{(i)}_{rz}(r, -t/2) - \tau^{(i+1)}_{rz}(r, t/2) = 0 \tag{12}$$

where $\tau^{(i)}_{rz}(r, -t/2)$ and $\tau^{(i+1)}_{rz}(r, t/2)$ are the bonding shear stresses generated by the elastic layers bonded to the top and bottom of the reinforcement i, respectively. From Eqs. (1) and (2), the shear stress $\tau^{(i)}_{rz}(r, z)$ of the elastic layer i has the form

$$\tau^{(i)}_{rz}(r, z) = \frac{\mu}{t}\left[\bar{u}^{(i)}(r)\left(-8\frac{z}{t}\right) + u^{(i-1)}_f(r) - u^{(i)}_f(r)\right] \tag{13}$$

Substituting Eqs. (10), (11), (13) into Eq. (12) yields

$$\left(u^{(i)}_{f,r} + \frac{u^{(i)}_f}{r}\right)_{,r} = \frac{\alpha_1^2}{12}(-4\bar{u}^{(i+1)} - 4\bar{u}^{(i)} - u^{(i+1)}_f + 2u^{(i)}_f - u^{(i-1)}_f) \tag{14}$$

with

$$\alpha_1 = \sqrt{\frac{12\mu(1-v_f^2)}{E_f t_f t}} \tag{15}$$

When the bearing is subjected to axial compression, the compression stiffness of the elastic layer i is determined by the effective compression modulus defined as (Tsai and Lee, 1998)

$$E_c^{(i)} = -\frac{1}{\varepsilon_c^{(i)}}\left\{\frac{1}{\pi b^2}\int_0^b\int_0^{2\pi}\left[\frac{1}{t}\int_{-t/2}^{t/2}\sigma_{zz}^{(i)}(r,z)\,dz\right]r\,d\theta\,dr\right\} \tag{16}$$

The vertical stress has the form

$$\sigma_{zz}^{(i)} = -\frac{\lambda}{\kappa}p^{(i)} + 2\mu w_{,z}^{(i)} \tag{17}$$

from which the effective compression modulus becomes

$$E_c^{(i)} = 2\mu + \frac{2\lambda}{b^2\varepsilon_c^{(i)}\kappa}\int_0^b \bar{p}^{(i)} r\,dr \tag{18}$$

The normal stress of the elastic layer i in the r direction has the form

$$\sigma_{rr}^{(i)} = -\frac{\lambda}{\kappa}p^{(i)} + 2\mu u_{,r}^{(i)} \tag{19}$$

At the edge of the elastic layer i, the normal stress in the r direction is zero, i.e. $\sigma_{rr}^{(i)}(b,z) = 0$. Substituting Eq. (1) into Eq. (19) and integrating through the thickness of the layer, this boundary condition becomes

$$\frac{1}{\kappa}\bar{p}^{(i)}(b) = \frac{2\mu}{\lambda}\left[\frac{2}{3}\bar{u}_{,r}^{(i)}(b) + \frac{1}{2}u_{f,r}^{(i-1)}(b) + \frac{1}{2}u_f^{(i)}(b)\right] \tag{20}$$

At the edge of the reinforcement, the normal force in the r direction is zero, i.e. $N_{rr}^{(i)}(b) = 0$, which means, from Eq. (12),

$$u_{f,r}^{(i)}(b) + \frac{v_f}{b}u_f^{(i)}(b) = 0 \tag{21}$$

3. Bearings with monotonic deformation

The bearing with monotonic deformation assumes that the displacement functions in all the reinforcements are the same, so the displacements in all the elastic layers are the same, which means $u_f^{(i-1)}(r) = u_f^{(i)}(r) = u_f^{(i+1)}(r)$ and $\bar{u}^{(i)}(r) = \bar{u}^{(i+1)}(r)$. Then Eqs. (5) and (14) become

$$\frac{\bar{p}^{(i)}}{\kappa} = -\left[\frac{2}{3}\left(\bar{u}_{,r}^{(i)} + \frac{\bar{u}^{(i)}}{r}\right) + u_{f,r}^{(i)} + \frac{u_f^{(i)}}{r} - \varepsilon_c^{(i)}\right] \tag{22}$$

$$\left(u_{f,r}^{(i)} + \frac{u_f^{(i)}}{r}\right)_{,r} = -\frac{2}{3}\alpha_1^2\bar{u}^{(i)} \tag{23}$$

Substituting Eqs. (8) and (23) into the differentiation of Eq. (22) with respect to r yields

$$\bar{u}^{(i)}_{,rr} + \frac{1}{r}\bar{u}^{(i)}_{,r} - \left(\frac{1}{r^2} + \alpha_0^2 + \alpha_1^2\right)\bar{u}^{(i)} = 0 \tag{24}$$

for which the solution has the form

$$\bar{u}^{(i)}(r) = C_1 I_1(\beta_0 r) \tag{25}$$

with C_1 being a constant to be determined, I_i being the modified Bessel function of the first kind of order i, and

$$\beta_0 = \sqrt{\alpha_0^1 + \alpha_1^2} \tag{26}$$

Substituting Eq. (25) into Eq. (8), we have

$$\frac{\bar{p}^{(i)}(r)}{\kappa} = -\frac{2}{3}\alpha_0^2\left[C_1\frac{1}{\beta_0}I_0(\beta_0 r) + C_2\right] \tag{27}$$

with C_2 being an integration constant. Substituting Eqs. (25) and (27) into Eq. (22) gives

$$u_f^{(i)} = \frac{-2\alpha_1^2}{3\beta_0^2}C_1 I_1(\beta_0 r) + \left(\frac{\alpha_0^2}{3}C_2 + \frac{\varepsilon_c}{2}\right)r \tag{28}$$

The constants C_1 and C_2 can be solved by substituting Eqs. (25), (27), (28) into the boundary conditions in Eqs. (20) and (21), from which Eq. (27) becomes

$$\frac{\bar{p}^{(i)}}{\kappa} = \varepsilon_c^{(i)}\left\{1 - \left(\frac{\lambda}{\lambda+\mu}\right)\frac{1}{D_1}\left[\frac{\alpha_0^2}{2}I_0(\beta_0 r) + \frac{\alpha_1^2}{1+v_f}\left(I_0(\beta_0 b) - (1-v_f)\frac{I_1(\beta_0 b)}{\beta_0 b}\right)\right]\right\} \tag{29}$$

with

$$D_1 = \frac{\alpha_0^2}{\lambda+\mu}\left[\left(\frac{\lambda}{2}+\mu\right)I_0(\beta_0 b) - \mu\frac{I_1(\beta_0 b)}{\beta_0 b}\right] + \frac{\alpha_1^2}{1+v_f}\left[I_0(\beta_0 b) - (1-v_f)\frac{I_1(\beta_0 b)}{\beta_0 b}\right] \tag{30}$$

Substituting Eq. (29) into Eq. (18), the effective compression modulus of the elastic layers in the bearing with monotonic deformation $(E_c)_{mono}$ is derived as

$$(E_c)_{mono} = 2\mu + \frac{\mu\lambda}{\lambda+\mu} + \frac{\lambda^2(\lambda+2\mu)}{(\lambda+\mu)^2}\left(\frac{\alpha_0^2}{2D_1}\right)\left[I_0(\beta_0 b) - \frac{2I_1(\beta_0 b)}{\beta_0 b}\right] \tag{31}$$

As $\lambda = \infty$, the asymptotic value is

$$(E_c)_{mono} = 3\mu + 24\mu S^2\left(\frac{1+v_f}{\alpha_1^2 b^2}\right)\frac{\alpha_1 b I_0(\alpha_1 b) - 2I_1(\alpha_1 b)}{\alpha_1 b I_0(\alpha_1 b) - (1-v_f)I_1(\alpha_1 b)} \tag{32}$$

with S being the shape factor of the circular layer defined as

$$S = \frac{b}{2t} \tag{33}$$

Eq. (32) is the compression modulus of the elastic layer of incompressible material, of which the last term is the same as the solution presented by Tsai and Kelly (2001). The asymptotic value of Eq. (31) for $E_f = \infty$ is

$$E_c = 2\mu + \lambda - \frac{\lambda^2}{(\lambda+2\mu)\frac{\alpha_0 b I_0(\alpha_0 b)}{2I_1(\alpha_0 b)} - \mu} \tag{34}$$

which is the effective compression modulus of the elastic layer bonded between rigid plates (Tsai and Lee, 1998).

From Eq. (28), the displacement of the reinforcements is

$$u_f^{(i)} = \varepsilon_c^{(i)}\left(\frac{\lambda}{\lambda+\mu}\right)\frac{\alpha_1^2}{2D_1}\left\{-\frac{I_1(\beta_0 r)}{\beta_0}+\frac{r}{1+v_f}\left[I_0(\beta_0 b)-(1-v_f)\frac{I_1(\beta_0 b)}{\beta_0 b}\right]\right\} \tag{35}$$

Substituting Eq. (35) into Eqs. (10) and (11) gives the normal forces of the reinforcements

$$N_{rr}^{(i)} = \left(\frac{6\mu\lambda}{\lambda+\mu}\right)\frac{\varepsilon_c^{(i)}}{D_1 t}\left\{[I_0(\beta_0 b)-I_0(\beta_0 r)]-(1-v_f)\left[\frac{I_1(\beta_0 b)}{\beta_0 b}-\frac{I_1(\beta_0 r)}{\beta_0 r}\right]\right\} \tag{36}$$

$$N_{\theta\theta}^{(i)} = \left(\frac{6\mu\lambda}{\lambda+\mu}\right)\frac{\varepsilon_c^{(i)}}{D_1 t}\left\{\left[I_0(\beta_0 b)-v_f I_0(\beta_0 r)\right]-(1-v_f)\left[\frac{I_1(\beta_0 b)}{\beta_0 b}+\frac{I_1(\beta_0 r)}{\beta_0 r}\right]\right\} \tag{37}$$

4. Bearings with free ends

When analyzing the free-end bearing where both ends are free from any horizontal shear force, the elastic layers can be divided into two groups, exterior and interior. The exterior layers are the elastic layers at the top and the bottom of the bearing, while the interior layers are the other elastic layers. The exterior layer is different from the interior layer in the analysis because one side of a reinforcement bonded to the exterior layer is not subjected to any shear force.

The top of the reinforcing sheet 0 is free from shear force, i.e. $\tau_{rz}^{(0)}(r,-t/2)=0$ in Eq. (12) of $i=0$, so that the equilibrium equation of the reinforcement 0 in Eq. (14) of $i=0$ becomes

$$\left(u_{f,r}^{(0)}+\frac{u_f^{(0)}}{r}\right)_{,r} = \frac{\alpha_1^2}{12}(-4\bar{u}^{(1)}+u_f^{(0)}-u_f^{(1)}) \tag{38}$$

Since the elastic layers 1 and 2 are adjacent, it is reasonable to assume these two elastic layers have the same bulge deformations, i.e. $\bar{u}^{(2)}(r)\approx\bar{u}^{(1)}(r)$. The elastic layer 2 is an interior layer that can be assumed as monotonically deformed, i.e. $u_f^{(2)}(r)\approx u_f^{(1)}(r)$. Based on these approximations, the equilibrium equation of the reinforcement 1 in Eq. (14) of $i=1$ becomes

$$\left(u_{f,r}^{(1)}+\frac{u_f^{(1)}}{r}\right)_{,r} = \frac{\alpha_1^2}{12}(-8\bar{u}^{(1)}-u_f^{(0)}+u_f^{(1)}) \tag{39}$$

The combination of Eqs. (38) and (39) gives

$$\left[(u_f^{(0)}+u_f^{(1)})_{,r}+\frac{1}{r}(u_f^{(0)}+u_f^{(1)})\right]_{,r} = -\alpha_1^2\bar{u}^{(1)} \tag{40}$$

Differentiating Eq. (5) of $i=1$ with respect to r and then bringing in Eq. (8) of $i=1$ and Eq. (40) yields

$$\bar{u}_{,rr}^{(1)}+\frac{1}{r}\bar{u}_{,r}^{(1)}-\left(\frac{1}{r^2}+\alpha_0^2+\frac{3}{4}\alpha_1^2\right)\bar{u}^{(1)}=0 \tag{41}$$

for which the solution has the form

$$\bar{u}^{(1)}(r) = C_3 I_1(\beta_1 r) \tag{42}$$

with C_3 being a constant to be determined and

$$\beta_1 = \sqrt{\alpha_0^2 + 0.75\alpha_1^2} \tag{43}$$

Then, substituting Eq. (42) into Eq. (8) of $i = 1$, we have

$$\frac{1}{\kappa}\bar{p}^{(1)}(r) = -\frac{2}{3}\alpha_0^2\left[C_3\frac{1}{\beta_1}I_0(\beta_1 r) + C_4\right] \tag{44}$$

with C_4 being an integration constant. Substituting Eqs. (42) and (44) into Eq. (5) of $i = 1$ gives

$$u_f^{(0)} + u_f^{(1)} = -\frac{\alpha_1^2}{\beta_1^2}C_3 I_1(\beta_1 r) + \left(\frac{2}{3}\alpha_0^2 C_4 + \varepsilon_c^{(1)}\right)r \tag{45}$$

From Eq. (21), we have

$$u_{f,r}^{(0)}(b) + u_{f,r}^{(1)}(b) + \frac{v_f}{b}[u_f^{(0)}(b) + u_f^{(1)}(b)] = 0 \tag{46}$$

The constants C_3 and C_4 can be solved by substituting Eqs. (42), (44), (45) into the boundary conditions in Eq. (20) of $i = 1$ and Eq. (46), from which Eq. (44) becomes

$$\frac{\bar{p}^{(1)}}{\kappa} = \varepsilon_c^{(1)}\left\{1 - \left(\frac{\lambda}{\lambda+\mu}\right)\frac{1}{D_2}\left[\frac{\alpha_0^2}{2}I_0(\beta_1 r) + \frac{0.75\alpha_1^2}{1+v_f}\left(I_0(\beta_1 b) - (1-v_f)\frac{I_1(\beta_1 b)}{\beta_1 b}\right)\right]\right\} \tag{47}$$

with

$$D_2 = \frac{\alpha_0^2}{\lambda+\mu}\left[\left(\frac{\lambda}{2}+\mu\right)I_0(\beta_1 b) - \mu\frac{I_1(\beta_1 b)}{\beta_1 b}\right] + \frac{0.75\alpha_1^2}{1+v_f}\left[I_0(\beta_1 b) - (1-v_f)\frac{I_1(\beta_1 b)}{\beta_1 b}\right] \tag{48}$$

Substituting Eq. (47) into Eq. (18), the effective compression modulus of the elastic layer 1 is derived as

$$E_c^{(1)} = 2\mu + \frac{\mu\lambda}{\lambda+\mu} + \frac{\lambda^2(\lambda+2\mu)}{(\lambda+\mu)^2}\left(\frac{\alpha_0^2}{2D_2}\right)\left[I_0(\beta_1 b) - \frac{2I_1(\beta_1 b)}{\beta_1 b}\right] \tag{49}$$

As $\lambda = \infty$, the asymptotic value is

$$E_c^{(1)} = 3\mu + 24\mu S^2\left(\frac{1+v_f}{0.75\alpha_1^2 b^2}\right)\frac{\sqrt{0.75}\alpha_1 b I_0(\sqrt{0.75}\alpha_1 b) - 2I_1(\sqrt{0.75}\alpha_1 b)}{\sqrt{0.75}\alpha_1 b I_0(\sqrt{0.75}\alpha_1 b) - (1-v_f)I_1(\sqrt{0.75}\alpha_1 b)} \tag{50}$$

The elastic layer n at the bottom of the free-end bearing has the same effective compression modulus as shown in Eq. (49). The interior layers are assumed to be monotonically deformed and have the effective compression modulus shown in Eq. (31). The stiffness of the bearing can be obtained by adding the stiffness of the elastic layers in series. The effective compression modulus of the free-end bearing consisting of n elastic layers is

$$(E_c)_{\text{free}} = \frac{n}{\frac{2}{E_c^{(1)}} + \frac{n-2}{(E_c)_{\text{mono}}}} \tag{51}$$

Let E and v be the elastic modulus and Poisson's ratio of the elastic layer, respectively. The ratio of the elastic layer stiffness to the reinforcement stiffness γ is defined as

$$\gamma = \frac{Et(1-v_f^2)}{E_f t_f} \tag{52}$$

Eqs. (31) and (49) indicate that the normalized effective compression modulus E_c/E is a function of v, v_f, S and γ.

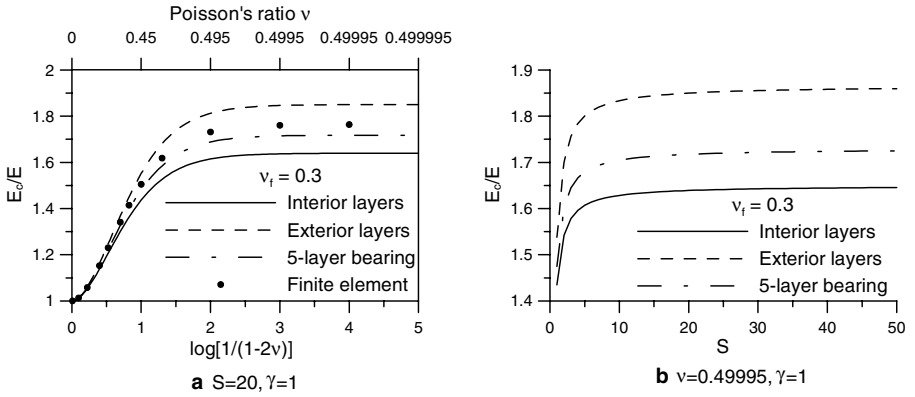

Fig. 3. Effective compression modulus of exterior layers and interior layers.

Fig. 3 compares the effective compression modulus in Eq. (31) for interior elastic layers, Eq. (49) for exterior elastic layers, and Eq. (51) for the free-end bearing consisting of five elastic layers. The results of finite element analysis for the five-layer bearing are also plotted in this figure. In the finite element analysis, each elastic layer is modeled by four layers of isoparametric 8-node axisymmetric elements. The reinforcement is modeled by one layer of isoparametric 6-node axisymmetric elements. This figure depicts that the stiffness of exterior layers is higher than the stiffness of interior layers. The effective compression modulus calculated from Eq. (51) is the closest curve to the finite element solution. The stiffness difference between the exterior layer and the interior layer becomes negligible when the stiffness ratio γ is very small. As shown in Eq. (51), $(E_c)_{free}$ becomes close to $(E_c)_{mono}$ when the number of elastic layers in the bearing, n, is large.

Variations of the effective compression modulus with Poisson's ratio ν and stiffness ratio γ are plotted in Figs. 4 and 5, respectively, for the free-end bearings consisting of 20 elastic layers. The theoretical solutions calculated from Eq. (51) are very close to the finite element solutions. The bearing with higher shape factor has a higher stiffness. The bearing stiffness increases with increasing Poisson's ratio ν. The bearing with high shape factor ($S = 20$) and high reinforcement stiffness ($\gamma = 0.01$) has a dramatic increase in stiffness when Poisson's ratio ν is near 0.5. The bearing stiffness decreases with decreasing the reinforcement stiffness (increasing γ). When $\gamma \to \infty$, the free-end bearing becomes an unbonded elastic block and its effective compression modulus approaches $E/(1-\nu^2)$ which is independent of the shape factor S.

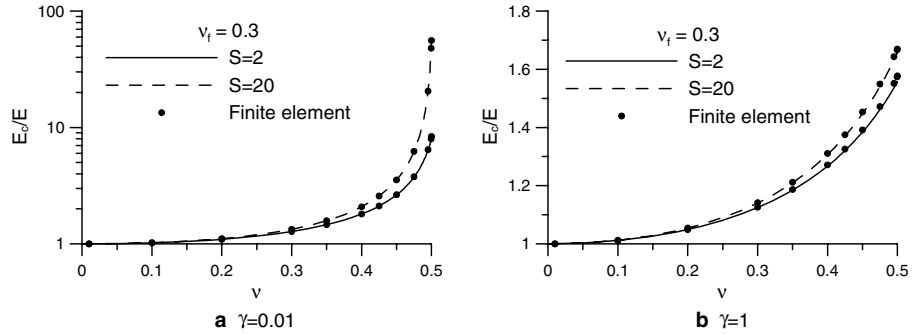

Fig. 4. Effective compression modulus varied with Poisson's ratio in 20-layer bearing with free ends.

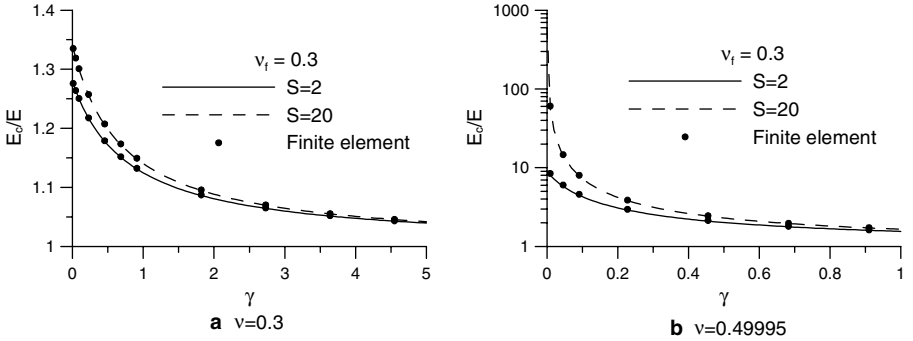

Fig. 5. Effective compression modulus varied with stiffness ratio in 20-layer bearing with free ends.

5. Bearings with rigid ends

For the bearing with rigid ends, the reinforcements at the ends of the bearings are subjected to rigid constraint, i.e. $u_f^{(0)}(r) = u_f^{(n)}(r) = 0$. When deriving the compression stiffness of the elastic layer i in the rigid-end bearing, the horizontal displacements of the reinforcements $i-1$, i and $i+1$ are assumed to be proportional to a displacement function $\tilde{u}^{(i)}(r)$, that is

$$u_f^{(i-1)}(r) = f_{i-1}\tilde{u}^{(i)}(r), \quad u_f^{(i)}(r) = f_i\tilde{u}^{(i)}(r), \quad u_f^{(i+1)}(r) = f_{i+1}\tilde{u}^{(i)}(r) \tag{53}$$

where f_i is a dimensionless quadratic function varied through the height of the bearing. For the bearing consisting of n elastic layers, f_i has the following form

$$f_i = 4\frac{i}{n}\left(1 - \frac{i}{n}\right) \tag{54}$$

Eq. (5) becomes

$$\frac{\bar{p}^{(i)}}{\kappa} = -\left[\frac{2}{3}\left(\bar{u}_{,r}^{(i)} + \frac{\bar{u}^{(i)}}{r}\right) + \frac{1}{2}(f_{i-1} + f_i)\left(\tilde{u}_{,r}^{(i)} + \frac{\tilde{u}^{(i)}}{r}\right) - \varepsilon_c^{(i)}\right] \tag{55}$$

By assuming $\bar{u}^{(i+1)}(r) \approx \bar{u}^{(i)}(r)$, Eq. (14) becomes

$$\left(\tilde{u}_{,r}^{(i)} + \frac{\tilde{u}^{(i)}}{r}\right)_{,r} = -\frac{2\alpha_1^2}{3f_i}\bar{u}^{(i)} + \alpha_{2i}^2\tilde{u}^{(i)} \tag{56}$$

with

$$\alpha_{2i}^2 = \frac{\alpha_1^2(-f_{i+1} + 2f_i - f_{i-1})}{12f_i} = \frac{2\alpha_1^2}{3n^2 f_i} \tag{57}$$

Substituting Eqs. (8) and (56) into the differentiation of Eq. (55) with respect to r yields

$$\tilde{u}^{(i)} = \frac{4}{3\alpha_{2i}^2(f_i + f_{i-1})}\left[-\left(\bar{u}_{,r}^{(i)} + \frac{\bar{u}^{(i)}}{r}\right)_{,r} + (\alpha_0^2 + \alpha_{3i}^2)\bar{u}^{(i)}\right] \tag{58}$$

with

$$\alpha_{3i}^2 = \frac{(f_i + f_{i-1})}{2f_i}\alpha_1^2 \tag{59}$$

Substituting Eq. (58) into Eq. (56) gives

$$\left[\left(\bar{u}^{(i)}_{,r}+\frac{\bar{u}^{(i)}}{r}\right)_{,rr}+\frac{1}{r}\left(\bar{u}^{(i)}_{,r}+\frac{\bar{u}^{(i)}}{r}\right)_{,r}\right]_{,r}-(\alpha_0^2+\alpha_{2i}^2+\alpha_{3i}^2)\left(\bar{u}^{(i)}_{,r}+\frac{\bar{u}^{(i)}}{r}\right)_{,r}+\alpha_0^2\alpha_{2i}^2\bar{u}^{(i)}=0 \tag{60}$$

for which the solution has the form

$$\bar{u}^{(i)}(r)=C_5I_1(\beta_{2i}r)+C_6I_1(\beta_{3i}r) \tag{61}$$

with C_5 and C_6 being constants to be determined, and

$$\beta_{2i}^2=\frac{1}{2}\left[\alpha_0^2+\alpha_{2i}^2+\alpha_{3i}^2-\sqrt{(\alpha_0^2+\alpha_{2i}^2+\alpha_{3i}^2)^2-4\alpha_0^2\alpha_{2i}^2}\right] \tag{62}$$

$$\beta_{3i}^2=\frac{1}{2}\left[\alpha_0^2+\alpha_{2i}^2+\alpha_{3i}^2+\sqrt{(\alpha_0^2+\alpha_{2i}^2+\alpha_{3i}^2)^2-4\alpha_0^2\alpha_{2i}^2}\right] \tag{63}$$

Substituting Eq. (61) into Eq. (58), we have

$$\tilde{u}^{(i)}=-\frac{4}{3\alpha_{2i}^2(f_i+f_{i-1})}[C_5(\alpha_0^2+\alpha_{3i}^2-\beta_{2i}^2)I_1(\beta_{2i}r)+C_6(\alpha_0^2+\alpha_{3i}^2-\beta_{3i}^2)I_1(\beta_{3i}r)] \tag{64}$$

Substituting Eqs. (61) and (64) into Eq. (55), we have

$$\frac{\bar{p}^{(i)}}{\kappa}=\varepsilon_c^{(i)}-\frac{2}{3}\alpha_0^2\left[C_5\frac{1}{\beta_{2i}}I_0(\beta_{2i}r)+C_6\frac{1}{\beta_{3i}}I_0(\beta_{3i}r)\right] \tag{65}$$

The constants C_5 and C_6 can be solved by substituting Eqs. (53), (61), (64) and (65) into the boundary conditions in Eqs. (20) and (21), from which Eq. (65) becomes

$$\begin{aligned}\frac{\bar{p}^{(i)}}{\kappa}=\varepsilon_c^{(i)}-\frac{\varepsilon_c^{(i)}}{D_3}\Bigg\{&\left(1-\frac{\alpha_{2i}^2}{\beta_{2i}^2}\right)\left[I_0(\beta_{3i}b)-(1-v_f)\frac{I_1(\beta_{3i}b)}{\beta_{3i}b}\right]I_0(\beta_{2i}r)\\&-\left(1-\frac{\alpha_{2i}^2}{\beta_{3i}^2}\right)\left[I_0(\beta_{2i}b)-(1-v_f)\frac{I_1(\beta_{2i}b)}{\beta_{2i}b}\right]I_0(\beta_{3i}r)\Bigg\}\end{aligned} \tag{66}$$

with

$$\begin{aligned}D_3=&\left[(1+\frac{2\mu}{\lambda})I_0(\beta_{2i}b)-\frac{2\mu}{\lambda}\frac{I_1(\beta_{2i}b)}{\beta_{2i}b}\right]\left(1-\frac{\alpha_{2i}^2}{\beta_{2i}^2}\right)\left[I_0(\beta_{3i}b)-(1-v_f)\frac{I_1(\beta_{3i}b)}{\beta_{3i}b}\right]\\&-\left[(1+\frac{2\mu}{\lambda})I_0(\beta_{3i}b)-\frac{2\mu}{\lambda}\frac{I_1(\beta_{3i}b)}{\beta_{3i}b}\right]\left(1-\frac{\alpha_{2i}^2}{\beta_{3i}^2}\right)\left[I_0(\beta_{2i}b)-(1-v_f)\frac{I_1(\beta_{2i}b)}{\beta_{2i}b}\right]\end{aligned} \tag{67}$$

Substituting Eq. (66) into Eq. (18), the effective compression modulus of the elastic layer i is derived as

$$\begin{aligned}E_c^{(i)}=2\mu+\lambda-\frac{2\lambda}{D_3}\Bigg\{&\left(1-\frac{\alpha_{2i}^2}{\beta_{2i}^2}\right)\left[I_0(\beta_{3i}b)-(1-v_f)\frac{I_1(\beta_{3i}b)}{\beta_{3i}b}\right]\frac{I_1(\beta_{2i}b)}{\beta_{2i}b}\\&-\left(1-\frac{\alpha_{2i}^2}{\beta_{3i}^2}\right)\left[I_0(\beta_{2i}b)-(1-v_f)\frac{I_1(\beta_{2i}b)}{\beta_{2i}b}\right]\frac{I_1(\beta_{3i}b)}{\beta_{3i}b}\Bigg\}\end{aligned} \tag{68}$$

As $\lambda = \infty$, the asymptotic value is

$$E_c^{(i)} = 3\mu + 6\mu S^2 \left\{ 1 - \frac{\alpha_{3i}^2}{\bar{\beta}_{3i}^2} \left[1 - \frac{4(1+\nu_f)}{\bar{\beta}_{3i}^2 b^2} \left(\frac{I_0(\bar{\beta}_{3i}b) - 2\frac{I_1(\bar{\beta}_{3i}b)}{\bar{\beta}_{3i}b}}{I_0(\bar{\beta}_{3i}b) - (1-\nu_f)\frac{I_1(\bar{\beta}_{3i}b)}{\bar{\beta}_{3i}b}} \right) \right] \right\} \tag{69}$$

with

$$\bar{\beta}_{3i}^2 = \alpha_{2i}^2 + \alpha_{3i}^2 \tag{70}$$

Adding the stiffness of each elastic layer in series can generate the effective compression modulus of the rigid-end bearing consisting of n elastic layers,

$$(E_c)_{\text{rigid}} = \frac{n}{\sum_{i=1}^{n} \frac{1}{E_c^{(i)}}} \tag{71}$$

It should be noted that the formula of $E_c^{(i)}$ in Eq. (68) is not suitable for $E_c^{(n)}$, because the equilibrium equation of the reinforcement i in Eq. (12) requires that the elastic layer $i+1$ has to exist below the reinforcement i, which is not applicable to the reinforcement n bonded to the elastic layer n at the bottom of the bearing. However, due to the symmetry of the loading, we have $E_c^{(n)} = E_c^{(1)}$.

Variations of the effective compression modulus with Poisson's ratio ν and stiffness ratio γ are plotted in Figs. 6 and 7, respectively, for the rigid-end bearings consisting of 20 elastic layers. The theoretical solutions calculated from Eq. (71) are very close to the finite element solutions. When the reinforcement stiffness is

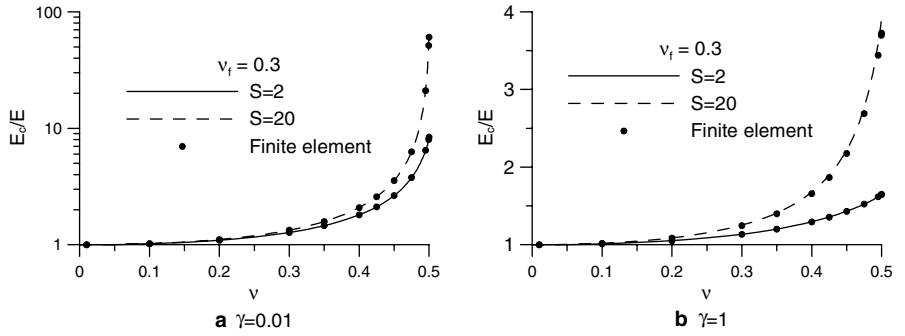

Fig. 6. Effective compression modulus varied with Poisson's ratio in 20-layer bearing with rigid ends.

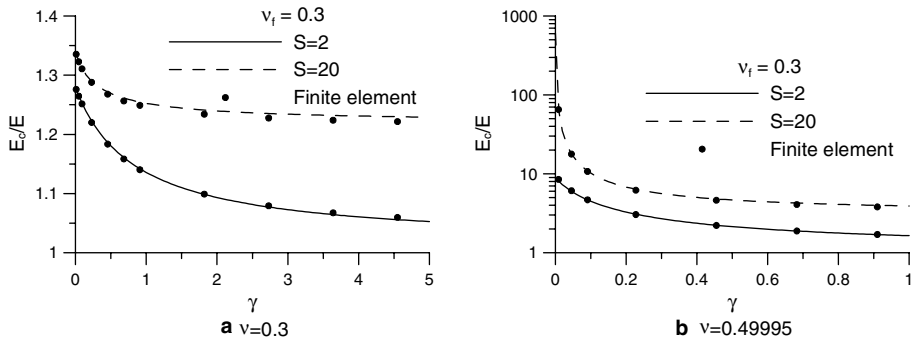

Fig. 7. Effective compression modulus varied with stiffness ratio in 20-layer bearing with rigid ends.

high ($\gamma = 0.01$), the stiffness of the rigid-end bearing is very close to the stiffness of the free-end bearing. When the reinforcement stiffness is low ($\gamma = 1$), the stiffness of the rigid-end bearing is higher than the stiffness of the free-end bearing because of the rigid constraint at the ends of the bearing. When $\gamma \to \infty$, the rigid-end bearing becomes an elastic block bonded by the rigid plates at the ends of the bearing and its effective compression modulus is dependent on the shape factor S and the number of elastic layers.

6. Conclusion

The closed-form solutions for the compression stiffness of the elastic layers bonded between flexible reinforcements in the circular bearings are derived. Because the compressibility effect of the elastic layers is considered in theoretical derivation, the closed-form solutions are accurate for the elastic layers of any Poisson's ratio. The boundary conditions of the bearings with flexible reinforcements can affect the bearing stiffness. Two types of the bearings are studied. One is the bearing with both ends being free from shear force. The other is the bearing with both ends being bonded to rigid plates. For the reinforcements of high stiffness, the boundary condition of the bearings has little influence on the bearing stiffness; the stiffness of the bearing has a dramatic increase when Poisson's ratio of the elastic layer is near 0.5, especially for the case of high shape factor. For the reinforcements of low stiffness, the behavior of the free-end bearing is similar to an unbonded elastic block, and its stiffness is independent of the shape factor of elastic layers; the behavior of the rigid-end bearing is similar to an elastic block bonded by rigid plates at the ends of the bearing, and its stiffness is dependent on the shape factor and the number of elastic layers.

The compression stiffness of the bearings calculated from the theoretical solution is extremely close to the result obtained from the finite element method, which proves that the displacement assumptions utilized in the theoretical derivation are reasonable. Using the finite element method to analyze the stiffness of multilayer bearings with flexible reinforcements is cumbersome. Furthermore, different sizes of bearings require different finite element meshes. Although the closed-form solutions presented in this paper involve the use of complex Bessel functions, the values of these functions can be easily calculated through mathematical program libraries. Therefore, these closed-form solutions provide a convenient way to establish computational program to calculate the stiffness of the bearings.

Acknowledgements

The National Science Council of Taiwan supported the research work reported in this paper under Grant No. NSC91-2211-E011-015. This support is greatly appreciated.

References

Chaihoub, M.S., Kelly, J.M., 1991. Analysis of infinite-strip-shaped base isolator with elastomer bulk compression. Journal of Engineering Mechanics, ASCE 117, 1791–1805.

Chaihoub, M.S., Kelly, J.M., 1990. Effect of bulk compressibility on the stiffness of cylindrical base isolation bearings. International Journal of Solids and Structures 26, 734–760.

Gent, A.N., Lindley, P.B., 1959. The compression of bonded rubber block. Proceeding of the Institution Mechanical Engineers 173, 111–117.

Gent, A.N., Meinecke, E.A., 1970. Compression, bending and shear of bonded rubber blocks. Polymer Engineering and Science 10, 48–53.

Kelly, J.M., 1997. Earthquake-resistant Design with Rubber, second ed. Springer-Verlag, London.

Kelly, J.M., 1999. Analysis of fiber-reinforced elastomeric isolator. Journal of Seismology and Earthquake Engineering 2, 19–34.

Kelly, J.M., 2002. Seismic isolation systems for developing countries. Earthquake Spectra 18, 385–406.
Kelly, J.M., Takhirov, S.M., 2002. Analytical and experimental study of fiber-reinforced strip isolators. PEER Report 2002/11, Pacific Earthquake Engineering Research Center, University of California, Berkeley.
Koh, C.G., Kelly, J.M., 1987. Effects of axial load on elastomeric isolation bearings. Report UCB/EERC-86/12, Earthquake Engineering Research Center, University of California, Berkeley.
Koh, C.G., Kelly, J.M., 1989. Compression stiffness of bonded square layers of nearly incompressible material. Engineering Structures 11, 9–15.
Koh, C.G., Lim, H.L., 2001. Analytical solution for compression stiffness of bonded rectangular layers. International Journal of Solids and Structures 38, 445–455.
Lindley, P.B., 1979a. Compression module for blocks of soft elastic material bonded to rigid end plates. Journal of Strain Analysis 14, 11–16.
Lindley, P.B., 1979b. Plane strain rotation module for soft elastic blocks. Journal of Strain Analysis 14, 17–21.
Tsai, H.-C., 2003. Flexure analysis of circular elastic layers bonded between rigid plates. International Journal of Solids and Structures 40, 2975–2987.
Tsai, H.-C., 2004. Compression stiffness of infinite-strip bearings of laminated elastic material interleaving with flexible reinforcements. International Journal of Solids and Structures 41, 6647–6660.
Tsai, H.-C., 2005. Compression analysis of rectangular elastic layers bonded between rigid plates. International Journal of Solids and Structures 42, 3395–3410.
Tsai, H.-C., Kelly, J.M., 2001. Stiffness analysis of fiber-reinforced elastomeric isolators, PEER Report 2001/05, Pacific Earthquake Engineering Research Center, University of California, Berkeley.
Tsai, H.-C., Kelly, J.M., 2002a. Stiffness analysis of fiber-reinforced rectangular seismic isolators. Journal of Engineering Mechanics, ASCE 128, 462–470.
Tsai, H.-C., Kelly, J.M., 2002b. Bending stiffness of fiber-reinforced circular seismic isolators. Journal of Engineering Mechanics, ASCE 128, 1150–1157.
Tsai, H.-C., Lee, C.-C., 1998. Compressive stiffness of elastic layers bonded between rigid plates. International Journal of Solids and Structures 35, 3053–3069.
Tsai, H.-C., Lee, C.-C., 1999. Tilting stiffness of elastic layers bonded between rigid plates. International Journal of Solids and Structures 36, 2485–2505.